MECHANICAL CHARACTERIZATION OF IRRADIATED FUEL MATERIALS WITH LOCAL ULTRASONIC METHODS

D. LAUX*[1], G.DESPAUX[1], D.BARON[2], J.SPINO[3]

[1] LAIN, Université Montpellier 2, 34095 Montpellier Cedex 05, France
[2] EDF/DER, Division Recherches et Développement, 77250 Moret/Loing, France
[3] ITU, Institut des transuraniens. Forschungszentrum Karlsruhe. Allemagne.

*Corresponding author : laux@lain.univ-montp2.fr

Since 1996, our research has been focused on the local assessment of mechanical properties of non-irradiated and irradiated fuels with micro-acoustic and micro-indentation [1] methods. In 1999, a study by acoustic microscopy concerning the influence of volume fraction porosity (in the range 1 to 7 %) on the elastic properties of non-irradiated fuel has been performed [2]. Other measurements on non-stochiometric samples containing Erbium and Cerium, and on irradiated pellets have proved all the potentiality of micro-acoustic approach [3]. This paper first deals with the improvement of the experimental ultrasonic device recently introduced in a hot cell in the Institute Für Transurane of Karlsruhe in order to get more local characterization or to operate on tiny samples. Secondly, measurements on very porous samples, Simfuel, and irradiated UO_2 pellets are presented and discussed.

1 - INTRODUCTION

Simulation codes used to predict the nuclear fuel rods thermo-mechanical behaviour in PWR have to evaluate in real time the local mechanical properties of the fuel. In particular, any change in volume fraction porosity can strongly modify these mechanical properties. Then, one has to find means to assess experimentally these parameters for different discharge burn-up. If classical ultrasonic methods are very accurate on non-irradiated fuel, they become inoperative on irradiated material because radial temperature and power gradients lead to a radial gradient in the evolution of the material and then of the local properties. Furthermore, due to the sharp radial temperature gradient, the integrity of the pellet is not preserved and a fracture pattern appears as soon as the irradiation starts, resulting in several random shaped pieces. So, techniques such as micro-indentation [1] and acoustic microscopy, which are able to perform mechanical characterisation on very small areas, can give new interesting approaches. Since 1996, the micro-indentation apparatus have been designed and realised in the ITU workshop. We have had to solve a lot of technical problems for such an apparatus designed to be used in hot cells, for samples between room temperature to 1200 °C. We expect the first data acquisition on nuclear fuel pellets before the end of this year.
We are already more advanced on the micro-acoustic device which is now in operation in the ITU hot cells since March 2001. Therefore, this paper will deal with this particular technique aiming

to present the state of art of it at this date.
As said here above, if measurements on non-irradiated fuel pellets can be performed with traditional acoustic microscopes, another methodology had to be implemented for irradiated cracked fuel pellets. This has been realised through the design and the construction of a specific acoustic microscope combined with a micro-echograph, introduced in the ITU hot cell.
As the irradiation proceeds in the nuclear fuel, its local physical-chemical state evolves depending on the local temperature and the local burn-up, due to the accumulation of fission products and irradiation defects (fission products in substitution, evolution of oxygen sub-lattice, creation of metallic or ceramic precipitates, lattice defects, porosity build-up or sintering, pellet cracking, grain restructuring, fission gas re-distribution or release...).
While, for non irradiated pellets, ultrasonic waves are only sensitive to the porosity relative volume, for irradiated fuel, all the parameters previously quoted are expected to have a more or less important influence. Consequently, the effect of each parameter on ultrasonic waves propagation should be quantified.
As such a study is not realistic, we propose to simplify the process dividing the effects in five major groups : porosity, Oxygen sub-lattice perturbation, metallic inclusions, trivalent fission products and tetravalent fission products. Each of these parameters has been studied in this paper. Thanks to measurements on Simfuel and simulations of metallic inclusions influence on ultrasonic waves, we show that only trivalent solid solutions, Oxygen sub-lattice perturbation and porosity are able to influence the elastic moduli. Furthermore, in PWR fuel, it seems that Oxygen potential does'nt evolves that much explained by the buffering of some species such as Molybdenum or Zirconium. As a consequence, one can expect that, via a small correction due to trivalent products, acoustic measurements can give immediately the volume fraction porosity and the local intrinsic elastic moduli (i.e. at zero percent porosity). Such data acquisition is useful to provide the 3D inverse methodology used to perform the identification of the mechanical laws parameters on micro-indentation tests.

2 - ASSESSMENT OF THE ELASTIC CONSTANTS FROM ULTRASONIC WAVES PROPAGATION VELOCITIES

Elastic moduli (Young and shear modulus) and Poisson ratio of an isotropic sample such as a sintered UO_2 material can be calculated from the knowledge of two measured ultrasonic velocities, using the relations (1) and (2) [4] :

$$E = \rho . V_t^2 \frac{3V_l^2 - 4V_t^2}{V_l^2 - V_t^2} \quad ; \quad G = \rho V_t^2 \qquad (1)$$

$$\sigma = \frac{E - 2G}{2G} \qquad (2)$$

In these expressions r ($Kg.m^{-3}$) is the density, E (Gpa) the Young modulus, G (Gpa) the shear

modulus, s the Poisson ration, V_t and V_l the transverse and longitudinal velocities of the ultrasonic waves in the material.
Except the longitudinal and transverse bulk waves, the theory of elastic sound propagation in solids shows that surface waves can propagate in some special conditions. The most well known of these surface waves is the Rayleigh one. Its velocity (V_r) is related to V_l and V_t with the expression (3) called Viktorov's formula [5] :

$$V_r = \frac{0.715 - 0.995\left(\frac{V_t}{V_l}\right)^2}{0.75 - \left(\frac{V_t}{V_l}\right)^2} V_t \qquad (3)$$

Experimentally V_l and V_r are measured and V_t is derived from (3). The traditional and new acoustic methods employed to measure V_l and V_r are described below. Our experimental device which has been introduced in hot cell in Karlsruhe is also presented.

3 - ULTRASONIC TECHNIQUES

3.1 - Acoustic microscopy [6]

Different information can be obtained on the mechanical properties of the sample. Acoustical pictures are acquired with an x-y scan performed on the sample with a spherical focused ultrasonic transducer. They give the variations of the coefficient of reflection which is a function of the density and the ultrasonic waves velocity. If the sensor is defocused, sub-surface structures, such as micro-cracks, can be visualized (an example is presented below). Although acoustical pictures only give qualitative information, quantitative results can be obtained with the acoustic signature so called V(z). In this operating mode, the spherical ultrasonic transducer is gradually defocused towards the sample. Interferences between surface waves and the specular ray create the pseudo-periodic signal V(z). On a theoretical point of view, three pseudo periods exist in the acoustic signature : the first is created by the longitudinal surface wave, the second by the transverse surface wave and the third by the Rayleigh wave. But, in most of case and especially on UO_2 only the periodicity (D_z) due to the Rayleigh wave is discernable. Then the Rayleigh wave velocity is calculated with the relation (4) :

$$V_r = \frac{V_{cf}}{\sqrt{1 - \left(1 - \frac{V_{cf}}{2F\Delta_z}\right)^2}} \qquad (4)$$

V_{cf} is the velocity in the coupling fluid present between the sample and the sensor and F (MHz) is the ultrasonic wave frequency. The latter governs the investigated area on the sample : higher is the frequency, smaller is the zone. In this paper two frequencies have been used: 15 and 140 MHz. The sizes analysed are respectively 1mm and 150 µm. On irradiated UO_2, because of attenuation, 200 MHz seems to be the highest reasonable frequency.

3.2 - Echography in reflexion/transmission mode

Difficulties to measure the longitudinal wave velocity can be overcome with micro-echography. Even if echography is well known in non-destructive testing, it is usually performed on a large zone in reflection mode. In this configuration, the time interval (Dt) between echoes reflected on the two parallel faces of the sample is measured. Then, if d is the thickness of the sample, the longitudinal velocity is calculated with the relation (5) :

$$V_l = \frac{2d}{\Delta t} \quad (5)$$

On irradiated UO_2 samples, operating in this mode is tricky because the ultrasonic waves have to propagate "2d" in the sample. Because of porosity and irradiation defects, the signal is very attenuated. Furthermore, knowing precisely "d" is impossible on fractured pellets. With the method so called micro-echography in transmission-reflection mode [7], "d" is accurately measured and the ultrasonic waves only propagate on a length "d" in the sample. A schema of the experimental device is given on figure 1. Calling 1 the ultrasonic wave travels through the water, 2 the ultrasonic wave travels in the sample, 3 and 4 the signals is reflected from the sample to the sensors, d and V_l are calculated as follows (Dt_{ij} is the time interval between signals i and j) :

$$d = \frac{V_{cf}(\Delta t_{13} + \Delta t_{14})}{2} \quad (6) \qquad V_l = \frac{d.V_{cf}}{d - \Delta t_{12}.V_{cf}} \quad (7)$$

The operating frequency is about 40 MHz and the analysed zone on the sample is 500 µm.

3.3 - Experimental device introduced in hot cell

The acoustic microscope introduced in an ITU hot cell is able to work both in acoustic microscopy and in micro-echographic mode. All the mechanical parts have been designed to be controlled by remote manipulators. A photograph of the device operating in acoustic signature mode is presented on figure 2.

4 - UO_2 PHYSICO-CHEMICAL PARAMETERS INVESTIGATION

4.1 - Effect of porosity in the range 1 to 20 %

The laws developed already by Vincent ROQUE in a porosity in the range 1 to 7 % , and

published in references [2] and [3], have been extended in the range 10 to 20 %. Such an extension was required for high porous zones study (fuel restructured areas for instance so called "rim"). Five batch of samples have been especially manufactured with relative porosity volumes of 10.1%, 12.08%, 12.33%, 14.81%, 20.04%. For each kind of sample, twenty measurements have been performed on five different pellets. Moreover, in acoustic signature mode, three ultrasonic frequencies (15, 50, 140 MHz) have been used. However, no significant variation has been observed on the Rayleigh wave velocity as a function of frequency. Furthermore, as mentioned in introduction, no important attenuation occurs, even on high porous samples. That is the reason why an increase in operating frequency should be possible on irradiated fuel : 200 MHz in V(z) and 100 MHz in micro-echography for example, in order to assess to more local characterisations. According to Mukhopadhyay and Phani [8] the longitudinal wave velocity can be fitted by laws such as $V_l=V_{lo}(1\text{-}ap)^b$ were a,b and V_{lo} have to be tuned on experimental data. Hence, for the evolution of the longitudinal velocity versus porosity, we propose the law (8) were p is the relative porosity volume (see figure 3).

$$V_l = 5465.(1-2{,}05p)^{\frac{2}{3}} \text{ or } \quad V_l \approx 5465.(1-1{,}37p-0{,}11p^2) \text{ for small values of p} \quad (8)$$

Concerning the Rayleigh wave velocity measurements, presented on figure 4, the best fit is given by the polynomial expression (9). Relation (10) gives the tuning of an equivalent polynomial expression for the evolution of V_t.

$$V_r = 2593(1-0{,}91p-0{,}68p^2) \quad (9)$$

$$V_t = 2770(1-0{,}77p-1{,}07p^2) \quad (10)$$

Then, with respect to the evolution of the density given by r=10960*(1-p), E, G and s have been calculated. Depending on material, many formulas can be proposed to fit the experimental data [9]. On our porous UO_2, the best polynomial fits are given by relations (11) and (12).

$$E = 223.(1-2{,}75p+0{,}82p^2)\,;\; G = 84.(1-2{,}56p+0{,}58p^2) \quad (11)$$

$$\sigma = 0{,}32-0{,}18p-p^2 \quad (12)$$

However, one must keep in mind that this kind of relation with porosity is also a function of the pore shape and their pressurisation. In this case, most of the porosity can be considered "relatively" spherically shaped and low pressurised. For high burn-up fuel, in the rim region one should have to account for the pore pressurisation. It can be done using a theoretical approach based on a multi-scaled homogeneisation methodology. For the pellet centre, it is again different as most of the porosity can be in the grain boundaries, low pressurised but with a lenticular shape. The theoretical approach will be also used to adapt the correlations.

* remark : we use here a density of 10960kg/m^3 because the samples are manufactured with depleted UO_2 powders with 0,2% ^{235}U enrichment. This value depend obviously upon the ^{235}U enrichment.

4.2 - Effect of Burn-up

a) Simulated influence of metallic precipitates

Models predicting the behaviour of two phase media [10], already applied to simulate the effect of porosity in our previous studies [2] have been used in the most general case to evaluate the effect of metallic fission products created during the fission process of Uranium. From [11] the main metallic inclusions are : Ru, Pd, Rh, Tc, Ag, Cd, Sn, Mo. These products represent about 25% of the fission products. As a result, for a burn-up of 5 % (nearly 50 GWd/tM), this constitute a concentration of 3% of metallic products in UO_2. Since there are ten types of inclusions, the concentration of each product is less than 1%. V_r has been evaluated in the range 0 to 10 %. The result is plotted on figure 5. The effect of Rh and Tc is not plotted because we do not have at this stage their mechanical constants, which are essential for the model. The mean effect of these precipitates is very small especially in the range 0 to 1 %. The same result can be demonstrated on V_l, E and G. Hence, the effect of metallic fission products can be neglected for small burn-up rates.

b) Experiments on Simfuel

In order to analyse out of pile the effect of high burn-up rates, simulated fuel (Simfuel) have been manufactured, by mixing solid "fission products" species with an UO_2 powder for contents representative of burn-up ranging from 25 to 215 Gwj/t. The samples used in this study have been previously manufactured by ITU and AECL to evaluate the evolution of the fuel conductivity with an increasing equivalent burn-up. One of these Simfuel has been prepared in Canada representative of a burn-up of 3% (or 25 GWj/t) [12]. The other pellets set has been manufactured in ITU : stoechiometric with a relative porosity volumes ranging between 2 and 4 %. For each of these samples we have measured V_r and reduced it to a value V_{ro} with 0% porosity, using the calibration laws established on pure UO_2. As the porosity is not accurately known an error must be accounted for on V_r evaluation. On these samples no assessment of V_l has been performed. But if we refer to pure UO_2, the ratio between V_l and Vr at 0 % porosity is 2,1. Hence, an evaluation of V_{lo} at 0% of porosity can be calculated. With such a procedure an estimation of E in obtained with 10 Gpa of mean error. Compared to UO_2 Young modulus, this leads to an error of 5%. The result is presented on figure 6. In this evaluation, the error is mainly due to the uncertainty on the porosity evaluation more than to the accuracy of the V_{lo} estimation. Indeed, with (1) and (3) one can show that an error of 100 $m.s^{-1}$ on V_l only creates an error of 1 Gpa on E.

In conclusion, if we take into account the accuracy of the evaluation, it appears that the effects of small and mean burn-up rates are very small compared the effect of the porosity presented here above.

In these experiments, all the interest of the local acoustic method has been demonstrated. Indeed, the ITU samples were inhomogeneous and fractured. This has been revealed with defocused acoustical pictures. Thanks to the local aspect of our methods, it has been possible focus the characterisation on non cracked areas. On figure 7, a comparison between optical and acoustical pictures is given.

4.3 - Effect of solid solutions

In 1999, B.Cros [3] has presented results on UO_2 with additives. The samples were non stoechimetric and highly porous:

Sample 1 : $(U,Ce)O_2$. %Ce = 50 %. O/M=2,2. p=2,5 %. Vr = 2404 $m.s^{-1}$
Sample 2 : $(U,Er)O_2$. %Er =10%. O/M=2,13. p=17 %. Vr = 2017 $m.s^{-1}$
Sample 3 : $(U,Er)O_2$. %Er =20%. O/M=2,06. p=22 %. Vr =1914 $m.s^{-1}$

With the recent acquisition obtained on high porosity pure UO_2 samples (up to 20 %) these results can be now refined. The Rayleigh wave velocities at 0 % porosity have been obtained using the relation (9). This respectively gives: 2461-2442-2495 $m.s^{-1}$. So, between the two samples containing Erbium, one can see that the main different parameter is the stochiometry. Indeed, the introduction of trivalent species in the UO_2 matrix modifies the Oxygen sub-lattice, creating Oxygen defects. This must results in a decrease of the elastic moduli and hence of the Rayleigh wave propagation velocity [13] [14]. Therefore, the last sample should have a smaller velocity than the second.
In fact, an inverse phenomenon is observed and can be related to the larger deviation from stochiometry of sample 2. Furthermore, one can expect that if tetravalent fission products effects were as important as effects of trivalent products, the velocity of the sample 1 should be very small.
This simple quantitative analysis shows that the effects of an addition of trivalent or tetravalent species, or the effect of a non-stochiometrique fabrication can be sorted as follow from the more influent to the less influent : initial O/M ratio, addition of trivalent species and addition of tetravelent species.
In PWR, the Oxygen potential doesn't vary that much because of the buffering by some metallic species such as Molybdenium or Zyrconium [15]. Therefore, the effects of trivalent fission products becomes the most important accounted for in the interpretation of the evolution of the ultrasonic wave propagation in the fuel material. Other measurements will have to be performed to had a correction factor related to this effect, in the previous calibration laws (8), (9), (10), (11) and (12) presented here above.

5 - IRRADIATED PELLETS STUDY

For this analysis we have used a sampling of a fuel rod irradiated in the BR3 reactor, similar to a standard PWR sample. The initial enrichment was 8.6 % ^{235}U and the average radial burn-up of the cross section used was 68 GWd/tU. Average initial grain size is 20 µm. The maximum burn-up at the pellet bore is 110 GWd/tU. During the first irradiation period the maximum linear rate has been nearly 300 W/cm. For the second half of the life, the average linear power rate has been representative of a standard PWR rod, not higher than 200 W/cm. Even if Xenon depletion has been observed in the very periphery of the fuel and pore have started to build-up in the rim region, a very few fuel restructuring has been observed. This has already been reported by SPINO

et al [16] in the JNM.
This sample, prepared in ITU has been studied both with acoustics and optics. A large 140 MHz picture on the whole pellet is presented on figure 8. This picture reveals three concentric zones. Acoustic signatures have been performed at 15 and 140 MHz. With the 15 MHz acoustic sensor, no significant variation of velocity has been observed because the zone analysed on the sample is too large. The mean Rayleigh wave velocity found is 2470 $m.s^{-1}$. The corresponding volume fraction porosity calculated with the calibration law is 5,5 %. This value can be interpreted as a mean porosity value on the pellet.
With the 140 MHz sensor, important variations appear on the Rayleigh wave velocity in the different zones. Using our calibration laws, the local porosity has been calculated. The results have been reported on figure 8. This results have also been compared to these obtained by optical analysis (Figure 9). The porosity evaluated by micro-acoustic methods seems slightly high but one must take in consideration that this methodology accounts for the overall porosity, even the porosity which is not detected by image analysis. An other aspect to be considered is that at this stage, no correction due to fission products has been made Obviously, the improvements expected in the near future to account for the effect of the trivalent fission products in solution will likely allow to increase the accuracy of the method.

6 - CONCLUSIONS

Physical-chemical parameters influence on elastic constants have been investigated with local acoustic methods. We have shown that only porosity and trivalent fission products have a major influence on elastic moduli in PWR fuel. Thanks to the improvement of the experimental device and the introduction of the apparatus in a hot cell, measurements on irradiated fuel have been started. The radial variation of porosity on a 68 GWj/t pellet has been measured and compared to optical study. Even if the porosity looks over-estimated, its variation along the pellet radius has been accurately measured. Extra characterisations planned in the near future on UO_2 containing additives should be implemented to correct the calibration laws presented in this paper and in particular take into account the effect of trivalent fission products. With these correlations, the ratio between V_l and V_r will be exactly known for each important parameter (porosity and trivalent products concentration). Since the influence of V_l on the Young modulus is very small, we will be able to measure the Young modulus only on a V_r assessment. Such an element is important because cutting the sample with to parallel faces for micro-echography is not an easy task ; it is obviously better if it can be avoided .

ACKNOLEDGEMENTS

The authors acknowledge M.Schreiber and M.Rousseau for their useful help to obtain the apparatus to be in operation in the ITU hot cells, for providing and preparing the samples used for this study, mainly the BR3 fuel samples . They also acknowledge Dr J-M Gatt for the useful discussions about the porosity effect on the fuel mechanical properties.

REFERENCES

[1] D.BARON, S.LECLERCQ, J.SPINO, S.TAHERI, « Development of a microindentation technique to determine the Fuel Mechanical Behaviour at High Burn-up », paper 6.6, IAEA TCM on Advances in Pellet Technology for Improved Performance at High Burn-up, Tokyo, Octobre 28th to Novembre 1st , 1996

[2] V.ROQUE, B.CROS, D.BARON, P.DEHAUDT, "Effect of the porosity in uranium dioxyde on microacoustic and elastic properties" J.Nuclear Materials, 277, 211-216 (2000).

[3] B.CROS, D.BARON, V.ROQUE, "Microacoustic techniques to assess to local characteristics of irradiated fuel materials", 6th International Conference on CANDU Fuel. Sept 26th-30th 1999, Niagara Falls, Canada.

[4] G.S.KINO, "Acoustic waves", Prentice-Hall, Inc. New Jersey (1987).

[5] I.A. VIKTOROV, "Rayleigh and Lamb waves", Plenum, New York (1967).

[6] A.BRIGGS, "Acoustic microscopy", Clarendon, Oxford (1992).

[7] D.LAUX, B.CROS, G.DESPAUX, D.BARON, "Ultrasonic study of UO_2 : effect of porosity and grain size on ultrasonic attenuations and velocities", submitted to J. Nuclear Materials.

[8] A.K. MUKHOPADHYAY, K.K. PHANI, "An analysis of microstructural parameters in the minimum contact area model for ultrasonic velocity-porosity relations". J. European Ceramic Society.20, 29-38 (2000).

[9] A .R. BOCCACCINI, Z. FAN, "A new approach for the Young's Modulus-Porosity Correlation of Ceramics Materials". Ceramics International. 23, 239-245 (1997)

[10] J.G.BERRYMAN, "Long wave propagation in composite elastic media I. Ellipsoïdal inclusions", J.Acoust.Soc.Am. 68, 6 (1980).

[11] H.BAILLY, D.MENESSIER, C.PRUNIER, "Le combustible nucléaire des réacteurs à eau sous pression et des réacteurs à neutrons rapides", CEA, Série synthèses (1996).

[12] P.G.LUCUTA, R.A.VERRALL, Hj.MATZKE, B.J.BALMER, "Microstructural features of SIMFUEL-Simulated high-burnup UO_2-based nuclear fuel", J.Nuclear Materials 178, 48-60 (1991).

[13] D.BARON, B.MESLIN, "Effet de l'adjonction de Gadolinium sur le comportement thermomécanique du combustible REP" EDF/DER. (1996).

[14] R.H.WATSON, "NFIR-Properties of the Urania-Gadolinia System (Part 2)", NFIR-RP04 (Final report) (March 1987).

[15] K.PARK, M.S. YANG, H.S. PARK, "The stoechiometry and the oxygen potential change of urania fuels during irradiation", J.Nuclear Materials 247, 116-120 (1997).

[16] J. Spino, D.Baron, M.Coquerelle, A.D.Stalios, J. Nucl. Mater. 256 (1998) 189

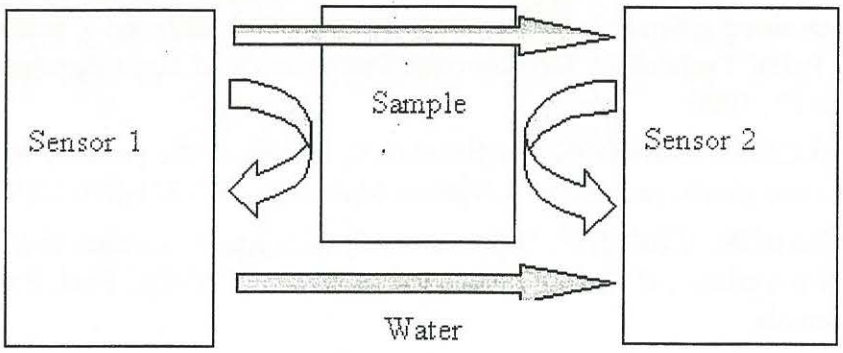

FIG.1 – MICRO-ECHOGRAPHY IN TRANSMISSION/REFLECTION MODE

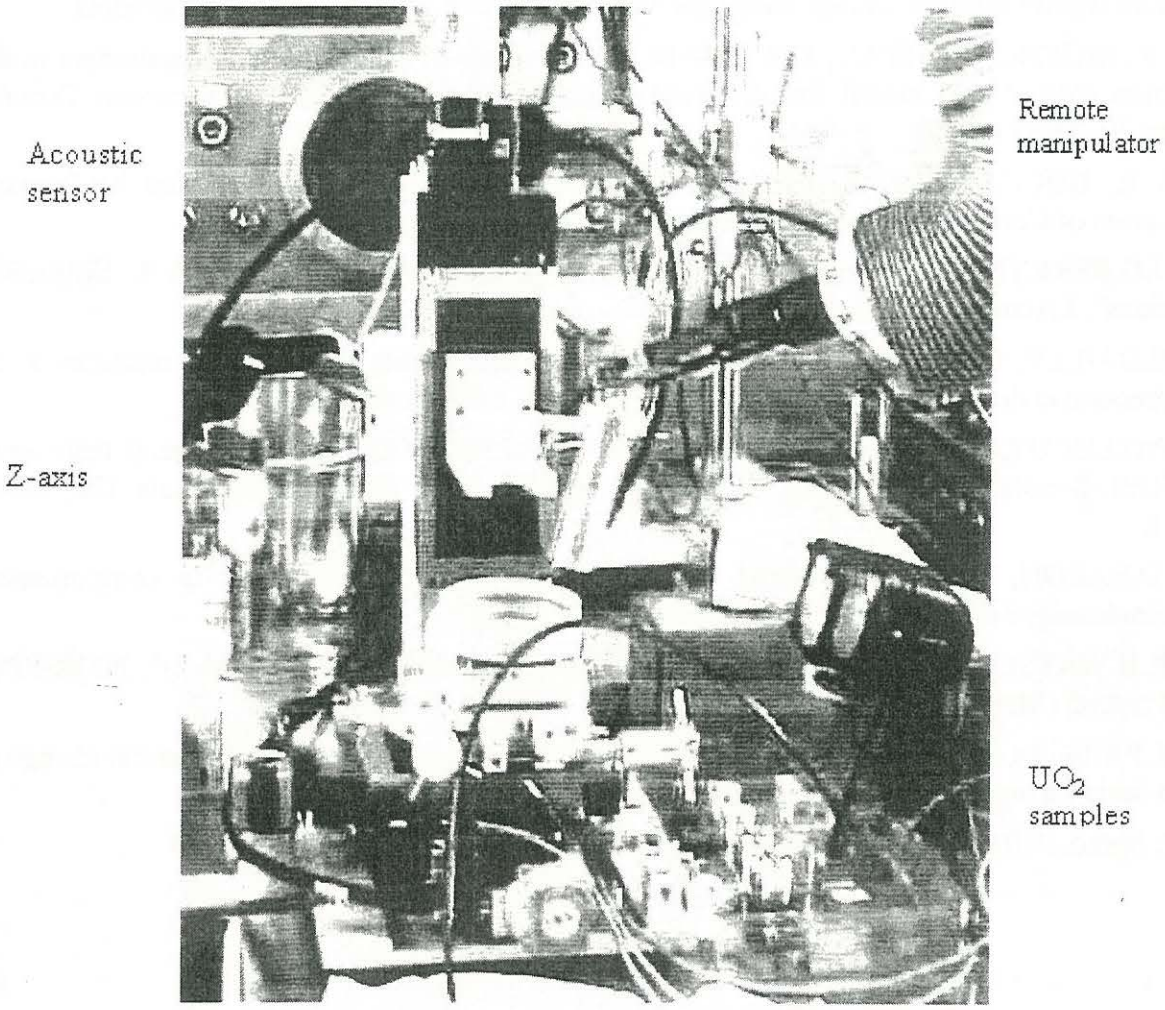

FIG.2 – EXPERIMENTAL DEVICE INTRODUCED IN HOT CELL

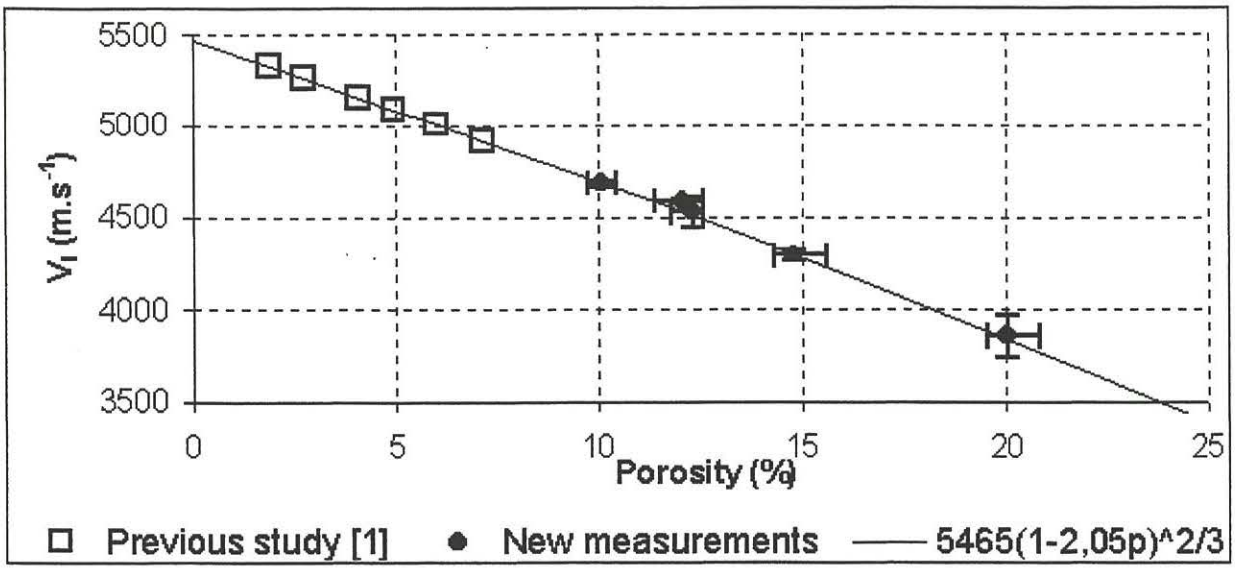

FIG.3- V_l MEASUREMENTS ON HIGH POROUS UO_2

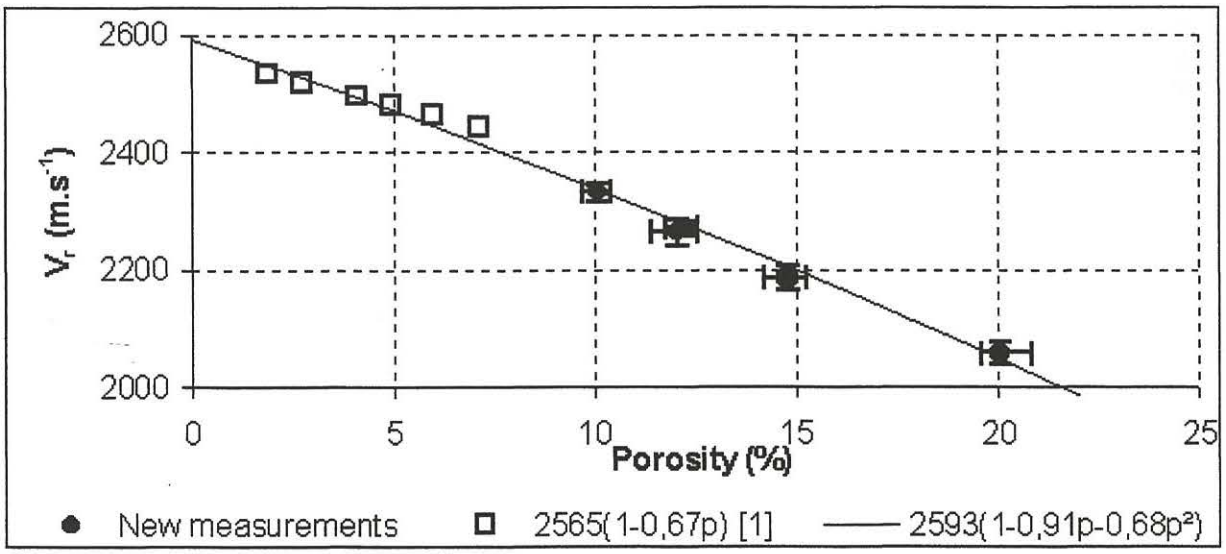

FIG.4- Vr MEASUREMENTS ON HIGH POROUS UO_2

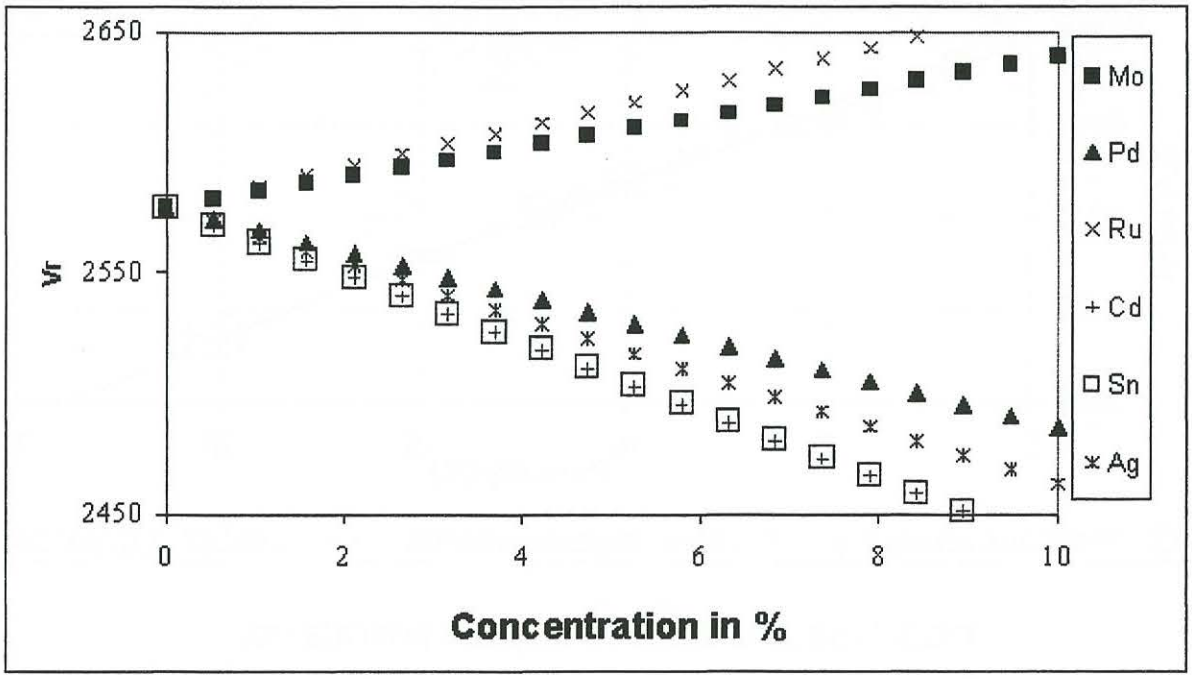

FIG.5- SIMULATED INLUENCE OF METALLIC FISSION PRODUCTS

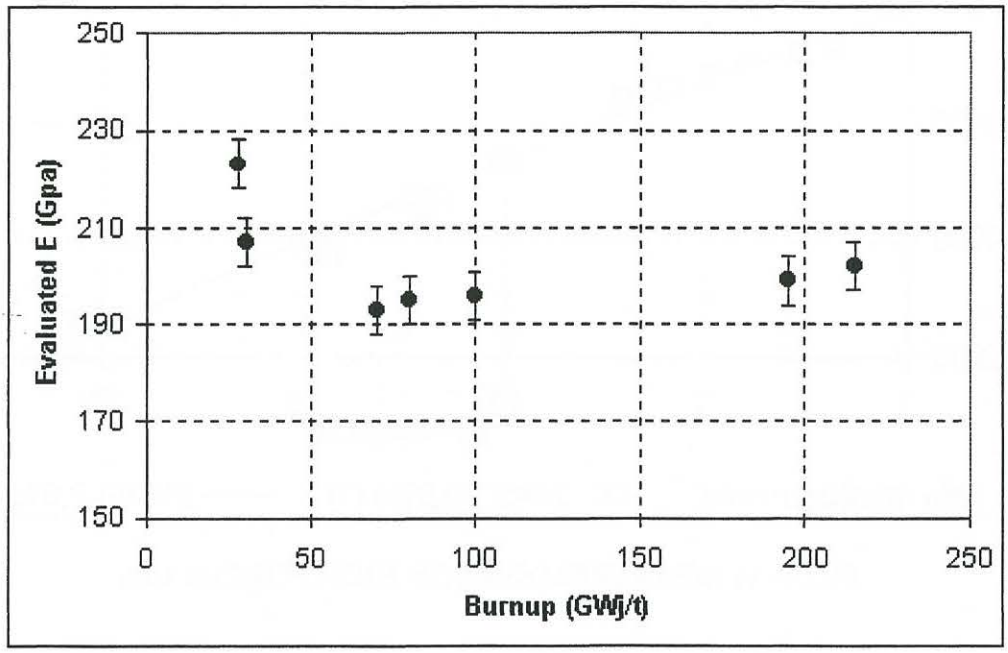

FIG.6-EVALUATION OF E(Gpa) ON SIMFUEL

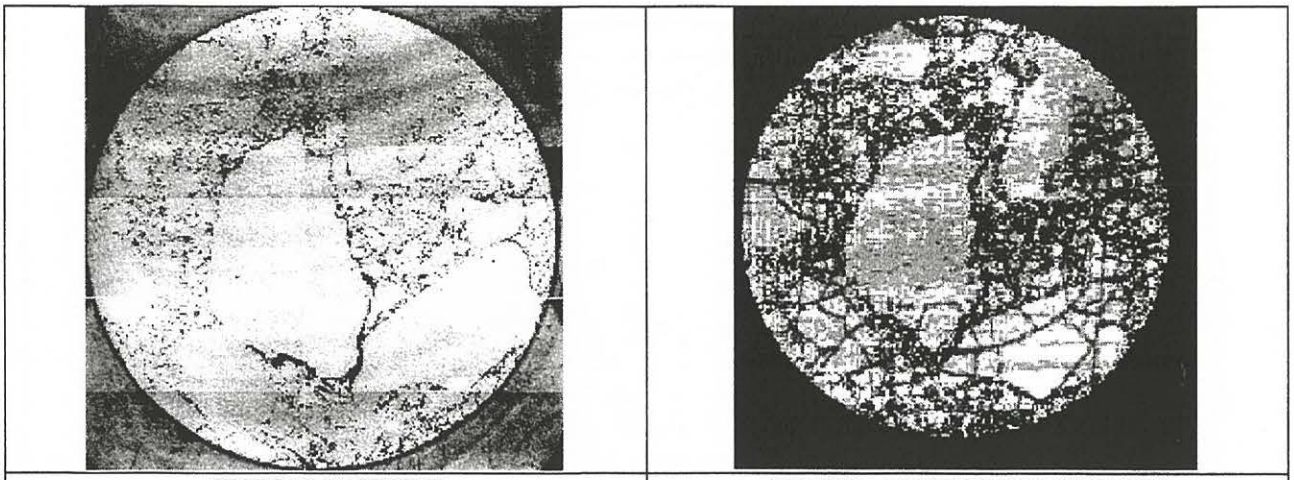

OPTICAL PICTURE	140 MHz ACOUSTICAL PICTURE

FIG.7- ACOUSTICAL VIZUALISATION OF CRACKS ON A 195 GWj/t SIMFUEL
SIZE (1 cm x 1 cm)

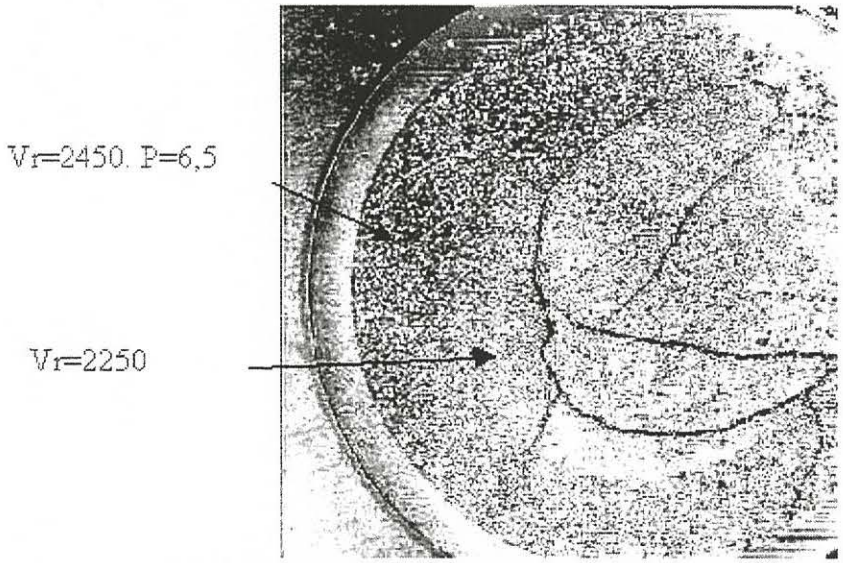

FIG.8 – 140 MHz ACOUSTICAL PICTURE ON A 67 GWd/tM UO_2 FUEL PELLET
(N118 fuel rod irradiated in the BR3 experimental core)

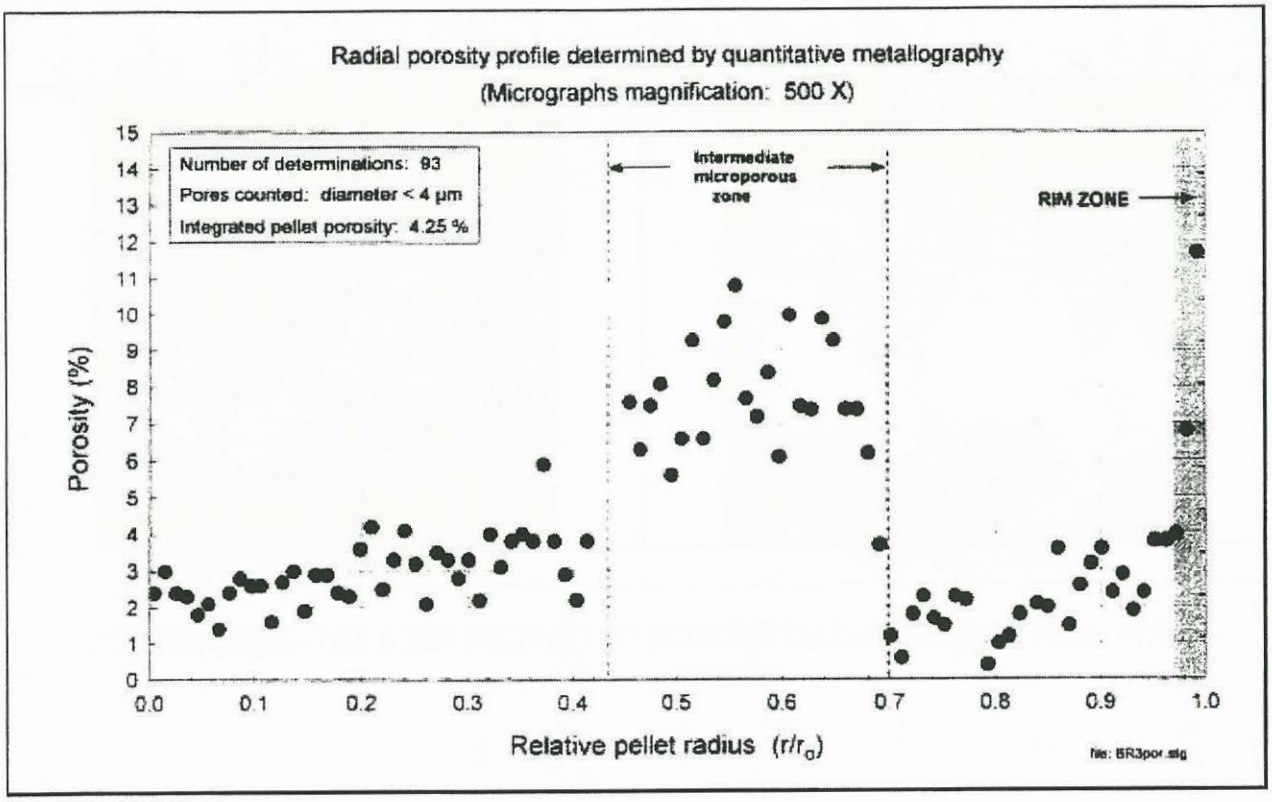

FIG 9 –Radial porosity profile in the N118 sample, 67 GWd/tM average